J Mater Sci: Mater Electron (2017) 28:7292–7301
DOI 10.1007/s10854-017-6414-8

CrossMark

Effect of temperature and substrate on shear strength of the joints formed by sintering of micro-sized Ag particle paste without pressure

Myong-Hoon Roh[1] · Hiroshi Nishikawa[1] · Seiichiro Tsutsumi[1] · Naruhiko Nishiwaki[2] · Keiichi Ito[2] · Koji Ishikawa[2] · Akihiro Katsuya[2] · Nobuo Kamada[3] · Mutsuo Saito[3]

Received: 3 August 2016 / Accepted: 17 January 2017 / Published online: 3 February 2017
© Springer Science+Business Media New York 2017

Abstract The production of joints using micro-sized Ag particle paste without applied pressure was investigated for replacing high lead containing solder in power electronic packaging. The micro-sized Ag paste used in this study was composed of chestnut-burr-like and spherical particles whose weight ratio was 5:5. Sintering was conducted at 250–400 °C for 60 min in a nitrogen atmosphere. Electroless nickel immersion gold (ENIG) finished Cu and bare Cu were used as the joint substrates. The experimental results showed that the microstructure at all sintering temperatures had an open porous system. The shear strength increased from 10.4 to 16.1 MPa with increasing sintering temperature from 250 to 300 °C, and there was no significant improvement above 300 °C. The Ag area ratio gradually increased with increasing sintering temperature, but the bonding ratio exhibited a similar trend to the shear strength. The ENIG finished Cu showed better bonding strength than bare Cu. The Ag area ratio of both substrates was almost similar but the bonding ratio on ENIG finished Cu (64.1%) was higher than that on bare Cu (40.9%).

✉ Myong-Hoon Roh
rohmh@nate.com

[1] Department of Smart Green Processing, Joining and Welding Research Institute, Osaka University, 11-1 Mihogaoka, Ibaraki, Osaka 567-0047, Japan

[2] NHK SPRING CO., LTD., 3-10 Fukuura Kanazawa-Ku, Yokohama 236-0004, Japan

[3] KAKEN TECH Co. Ltd., 901 Shimofutamatacho, Higashiomi, Shiga 527-0065, Japan

1 Introduction

Silver (Ag) is an attractive material as an alternative to high lead-containing solder for power electronic packaging due to its low temperature sinterability and high melting temperature after bonding. Also, Ag is a metal with good electrical and thermal conductivity [1–4]. Since the low temperature sintering technique by micro-sized Ag paste under applied pressure was tried by Schwarzbauer for die attach joints [5], Ag nanoparticle paste has been studied for reducing the applied pressure during sintering [6–10]. Compared to pressure sintering, pressureless sintering can avoid any potential harm to the chip and be more easily applied to the conventional joint process.

Although Ag nanoparticle paste has been developed for pressureless sintering, few studies have reported Ag joint with proper shear strength compared to conventional Pb-base solder [6–8]. Yan et al. fabricated Ag joint with a shear strength of more than 20 MPa using a 40 nm average diameter nanoparticle [6]. Wang et al. achieved a high shear strength of Ag joint by thinning the organic shells on Ag nanoparticles [7]. In both the studies, a high Ag content of 96.1 and 97.5 wt% in paste enabled the high-strength of the Ag joint despite the difference of their bonding variables such as a particle size, joint area, and sintering conditions. Wang et al. also investigated the sinterability of Ag nanoparticle paste with Ag content of 82 wt% [8]. They reported Ag joint with a shear strength of about 20 MPa by optimizing the sintering conditions. These studies had in common that Ag coated Cu was used as a substrate.

It is well known that a Ag coated substrate is easily bonded by a Ag nanoparticle paste due to the similar chemistry and lattice constant between substrate and paste [11]. Akada et al. reported that Au coated substrate also showed good bondability with Ag nanoparticle paste [12].

The comparable lattice constants between Au (0.4079 nm) and Ag (0.4086 nm) were helpful, and the epitaxial growth of Ag on the Au surface was suggested as the reason the interfacial energy was reduced. Compared to Ag and Au, the lattice constant of Cu (0.3625 nm) is significantly different. Despite the lattice mismatch between Ag and Cu, Ag joints on bare Cu substrates with high bonding strength in pressure sintering were reported by various researchers [12–14]. However, in the case of pressureless sintering using bare Cu substrates, the shear strengths of Ag joints were in the range of 7–11 MPa [9, 10].

Several studies on formation of Ag joints with micro-sized Ag particle paste have been reported [5, 15, 16]. These studies identified that applied pressure was needed during sintering. Low-pressure sintering using a mixed paste of micro-sized Ag flake and sub-micron Ag particles was attempted for die attachment [17]. With similar mixed Ag paste, a small area joint of 600 μm^2 by pressureless sintering was also investigated for die bonding of light-emitting diodes (LEDs) [18]. However, with the exception of our previous study [19], there are no reports about pressureless bonding using only micro-sized Ag particle paste for high temperature power electronic packaging. The pressureless process is applicable to various fields in electronic packaging and using micro-sized Ag particle paste, it is possible to get comparable cost efficiency to Ag nanoparticle paste. Therefore, Ag paste composed of only micro-sized particles was suggested for pressureless sintering and the effect of sintering temperature and bonding substrate on shear strength was investigated in this study. In addition, the bonding strength was studied in correlation with the microstructure, fracture properties, and interfacial reaction of the Ag joint sintered with the micro-sized Ag particle paste.

2 Experimental procedures

The micro-sized Ag paste provided by KAKEN TECH Co. Ltd., (Shiga, Japan) was prepared for pressureless sintering. The paste composed of a glycol ether-base solvent, Ag particles, and minor SiO_2 particles. The paste had a metal content of 86 mass%. The micro-sized Ag particles were consisted of chestnut-burr-like (CBL) particles with an average diameter of 3 μm and spherical particles having an average diameter of 1.5 μm. The weight ratio of CBL and spherical particles was 5:5. The morphology of Ag paste dried for 24 h at room temperature in air is shown in Fig. 1.

Two kinds of Cu disks were used as bonding substrates. One was a bare Cu disk (oxygen-free, 99.99%) and the other was metalized with electroless nickel immersion gold (ENIG-finished Cu). The dimensions of the top and bottom Cu disks were 3 mm (Φ)×2 mm (t) and 10 mm (Φ)×5 mm (t), respectively. Before bonding, the Cu disks were immersed in hydrochloric acid, and rinsed with ethanol solution. ENIG-finished Cu disks were cleaned with ethanol solution. The Ag paste was printed onto the bottom Cu substrate using a stainless steel metal mask (Φ=5 mm, t=150 μm), and the smaller Cu disk was set on top of it. A schematic diagram of sample alignment is presented in Fig. 2a. The prepared specimen with ENIG-finished Cu was pre-heated at 130 °C for 5 min and sintered at 250–400 °C for 60 min in a nitrogen atmosphere without

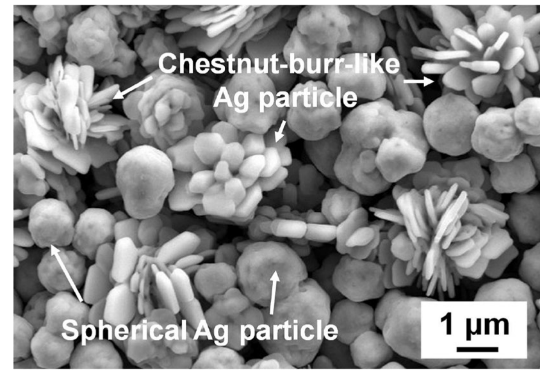

Fig. 1 Morphology of micro-sized Ag paste composed with chestnut-burr-like and spherical particles

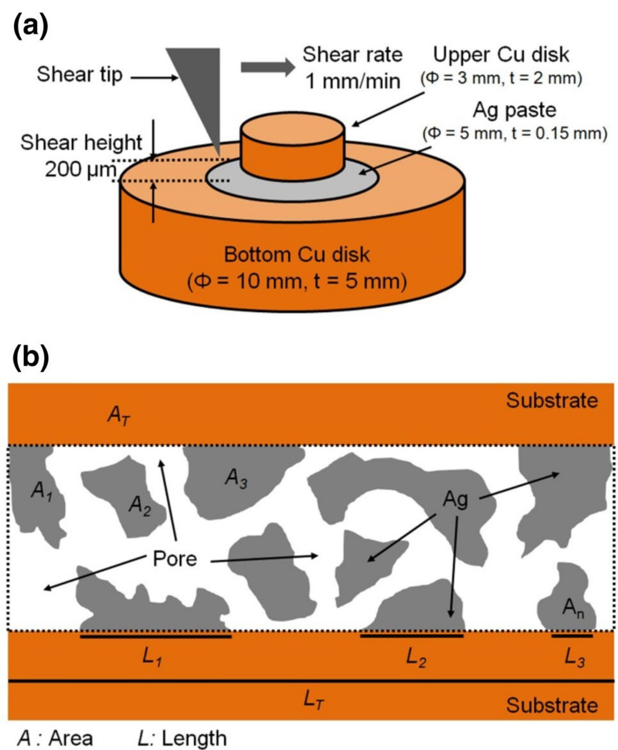

Fig. 2 **a** Schematics of specimen alignment for Cu/Cu joint and **b** the parameters for Ag area ratio and bonding ratio

pressure. Pre-heating was undertaken to evaporate the solvent. In order to confirm the effect of the substrate, a Cu to Cu joint was bonded at 300 °C with the same preheating and sintering process. Additionally, a formic acid atmosphere during preheating and sintering process was tried, to verify the effect of Cu oxidation on joint strength.

The morphology of Ag particles and the microstructure of the joints were observed by field emission scanning electron microscopy (FE-SEM, SU-70; Hitachi Ltd.) and electron probe micro-analysis (EPMA). The Ag area ratio and bonding ratio were measured for the quantitative analysis of the microstructure. The Ag area ratio (*A.R.*) and bonding ratio (*B.R.*) were calculated using a cross-section image of the joint and the following equations;

$$A.R.\,(\%) = \Sigma A_n/A_T \times 100 \quad (1)$$

$$B.R.\,(\%) = \Sigma L_n/L_T \times 100 \quad (2)$$

where A and L are the area and length of Ag, n is the number of Ag parts, and A_T and L_T are the total area and length of joint measured in the cross-section. The schematics of *A.R.* and *B.R* are shown in Fig. 2b. Shear strength of the joint was evaluated at a crosshead speed of 1 mm/min and a height of 200 µm using a shear tester (STR-1000, Rhesca Co.). Shear strength was calculated as a measured force divided the area of the top Cu dick.

3 Results and discussion

3.1 Effect of bonding temperature on shear strength of sintered joint

The surface morphologies of sintered Ag paste according to sintering temperature are shown in Fig. 3. The sintered Ag pastes at all temperatures had an open porous structure. Compared with the dried particles as shown in Fig. 1, the chestnut-burr-like particles were relatively rounded after heating. The connection between Ag particles was enhanced as the sintering temperature increased from 250 to 300 °C, but the effect of temperature appeared to be minimal after 300 °C. In the case of pressureless sintering by paste, it is difficult to achieve a dense structure because the particle packing in paste after screen printing has a more open state than the traditional plastic body [20]. According to the study of Lin et al. compared with free sintering, the sintering of Ag paste on a rigid substrate is constrained because the densification mechanism changes from grain-boundary diffusion to lattice diffusion [21]. As a result, the relative density of constrained sintering at 550–650 °C for 40 min was about 75–88%. Although the Ag area ratio was measured instead of relative density in this article, the area ratio of Ag paste sintered at 250–400 °C for 60 min was about 58–66% (see Fig. 4) and it showed a similar tendency with constrained sintering.

The shear strength, area ratio, and bonding ratio according to sintering temperatures are shown in Fig. 4. The ENIG finished Cu joint sintered at 250 °C had an average shear strength of 10.4 MPa and the others showed similar

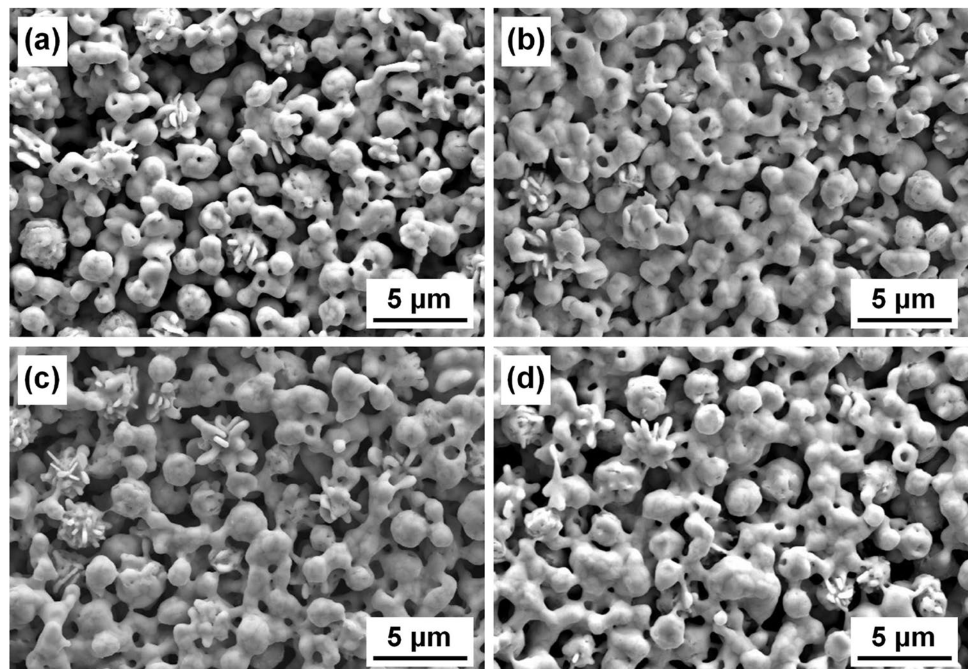

Fig. 3 SEM images of Ag paste after sintering according to bonding temperature at **a** 250 °C, **b** 300 °C, **c** 350 °C, and **d** 400 °C for 60 min

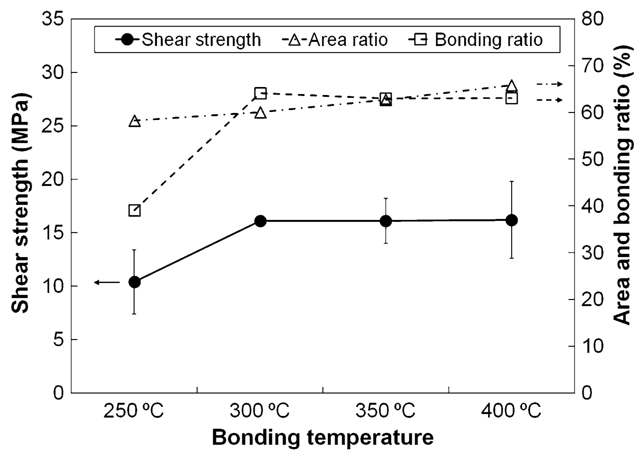

Fig. 4 Shear strength, area ratio, and bonding ratio of Ag paste sintered at different temperature using ENIG-finished Cu substrate

values of about 16 MPa. In the TG-DTA results of our previous study [19], an exothermic peak was observed at 250 °C, which indicated that additional decomposition of organic components on particle surfaces would have been in progress. This would not be helpful for Ag paste sintering in this study because organic components on particle surfaces interfere with the direct contact between the particles. However, it was observed that the shear strengths at 300–400 °C increased because sintering was performed after completion of the decomposition of organic components [8, 9]. On the other hand, the area ratio of Ag gradually increased from 58.3 to 65.8% with increasing temperature from 250 to 400 °C. In contrast, the bonding ratio showed the similar trend to the shear strength. Incomplete decomposition of the surface organic layer at 250 °C would interfere with bonding between Ag particles and the substrate. The bonding ratio exhibited an almost constant value of about 63% from 300 °C. Based on the relationship between the shear strength, area ratio, and bonding ratio, the shear strength was closely related to the bonding ratio rather than the area ratio. Although the shear strength corresponding to sintering above 300 °C is weaker than that of Pb-5mass%Sn solder (18 MPa) [2], it is enough for most practical applications because the joints are covered and strengthened by an encapsulating epoxy resin [9].

Figure 5 exhibits the typical cross-sections of joints sintered at 250 and 300 °C. As shown in Fig. 5, the respective bonding lengths of Ag particles sintered at 250 °C were shorter than those sintered at 300 °C, even though the number of Ag particles near the substrate was similar. The short bonding length means a small bonding area between Ag particle and substrate, and this can be a weak part of the fracture. Thus, the low bonding ratio is considered to be the cause of low shear strength of joint sintered at 250 °C.

Figure 6 shows the schematic illustrations of fracture position and the typical fracture surfaces according to the sintering temperature. In Fig. 6a, b, two fracture types depending on the fracture path were defined. Type 1 fracture is a failure between the sintered Ag particle and the substrate. Type 2 fracture is a failure between the sintered Ag particles. Type 1 and Type 2 fractures appear on the fracture surface as shown in Fig. 6c, d (white circle). The amounts of both fracture types on the fracture surface of joint sintered at 250 °C were similar, whereas there were a few Type 1 fractures on the fracture surfaces of joint sintered at 300–400 °C (see Fig. 6d–f). Since fracture generally occurs in a weak part, the reduction of Type 1 fracture indicates that the bonding between Ag particles and the substrate is enhanced as the sintering temperature increases.

Figure 7 presents the mapping data of interfaces sintered at different temperatures by EMPA. In the mapping results, it was observed that Au atoms diffused into sintered Ag in all joints. These diffusion behaviors showed the similar tendency in all joint parts, even though the sintered Ag had a porous structure. Generally, from the Ag–Au phase diagram, Ag and Au have an unlimited solid solubility and the solid-solution strengthening occurs due to the increased resistance to dislocation movement. Solid-solution strengthening of Ag–Au alloy was also reported and its critical shear stress increased until the amount of Au became 50 at.% [22]. Thus, solid-solution strengthening based on Au diffusion at the interface between Ag and substrate was expected and fractures between Ag and

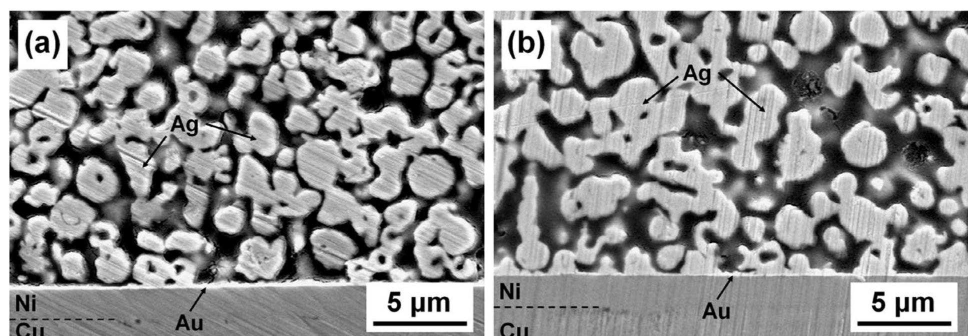

Fig. 5 Cross-section images of joints sintered at **a** 250 °C and **b** 300 °C

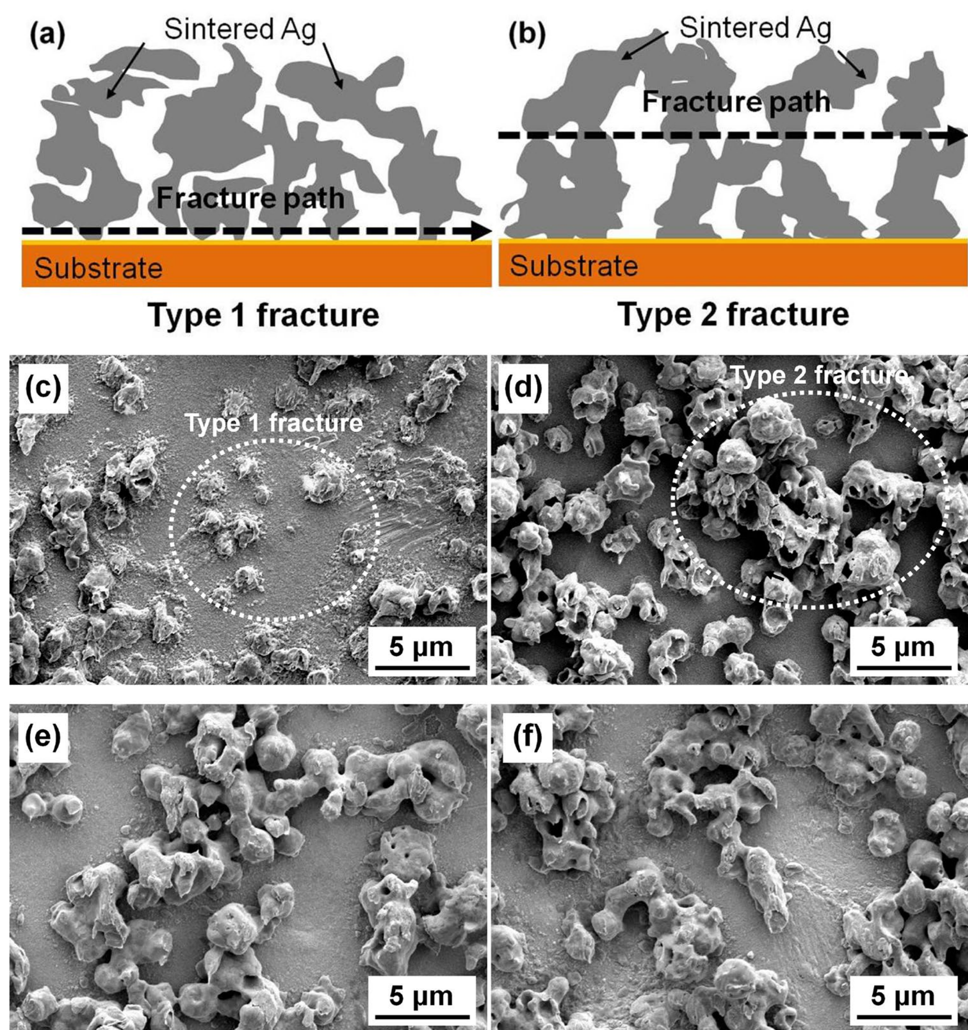

Fig. 6 Schematic illustrations and typical fracture surfaces of joints sintered at different temperatures. **a** Schematic of the type 1 fracture, **b** schematic of the type 2 fracture, the fracture surfaces of joints sintered at **c** 250 °C, **d** 300 °C, **e** 350 °C, and **f** 400 °C for 60 min

substrate occurred at the sintered Ag instead of the interface. In contrast, there was little diffusion of Ag and Ni into one another. According to a study by Kim et al. Ni layers which have generally been used as Cu diffusion barriers in Sn-based solder joints could have the same function as Ag and Au atoms because an amorphous Ni layer has very few diffusion paths (such as grain boundaries or dislocation) compared to a crystalline Ag matrix [23]. This study reconfirmed that the Ni layer worked as a Ag diffusion barrier up to sintering temperatures of 400 °C.

3.2 Effect of substrate on shear strength and microstructure of sintered joint

Figure 8 shows the effect on the shear strength of the Ag joint for different substrates sintered at 300 °C for 60 min under N_2 and formic acid atmospheres without applied pressure. The joint on ENIG finished Cu under N_2 and formic acid atmospheres had shear strengths of 16.1 and 15.9 MPa, respectively. The shear strengths of bare Cu joint under the same atmospheres were 10.4 and 11.2 MPa, respectively. It is well known that Ag pastes readily sinter not only on Ag surfaces but also on other noble metals, such as Au, Pd, and Pt. With regard to sintering of Ag nanoparticles to substrates, Hirose's group investigated the interfacial bonding mechanism by TEM analysis [12]. They reported that the epitaxial growth of Ag occurred on Au substrates because the lattice constants of Ag (0.4086 nm) and Au (0.4079 nm) were almost the same and this could reduce the interfacial energy. Also, although the lattice constants of Ag and Cu (0.3615 nm) are significantly different, Ag on Cu substrates showed a good joint strength due to a metallic bond between Ag and Cu atoms. From these results, they suggested that the bonding strength depended more on the sintered Ag layer than on the interface strength. Thus, in order to observe the fracture position, we conducted the surface analysis after the shear test.

Figure 9 presents the typical fracture surfaces observed by EPMA mapping on both ENIG and bare Cu substrates bonded in N_2. The top and bottom fracture surfaces of the

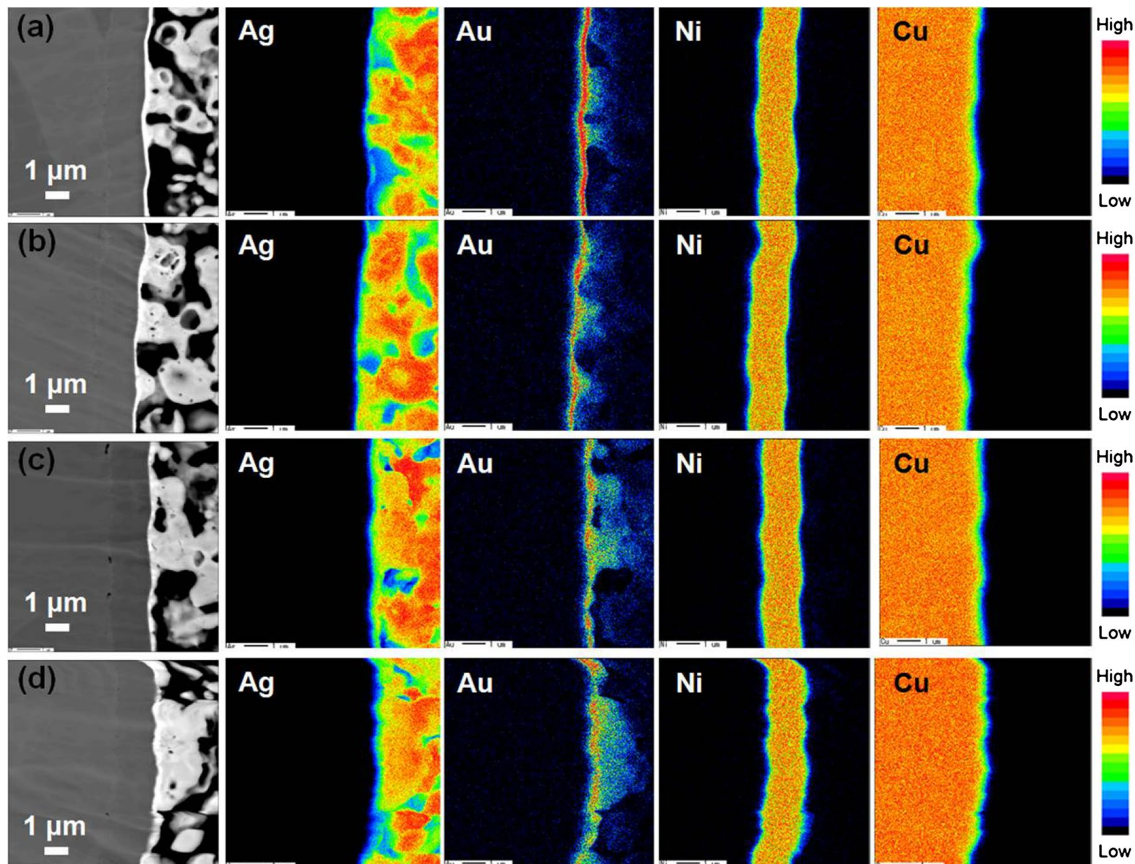

Fig. 7 EMPA results of joints between Ag and ENIG finished Cu substrate sintered at **a** 250 °C, **b** 300 °C, **c** 350 °C, and **d** 400 °C for 60 min

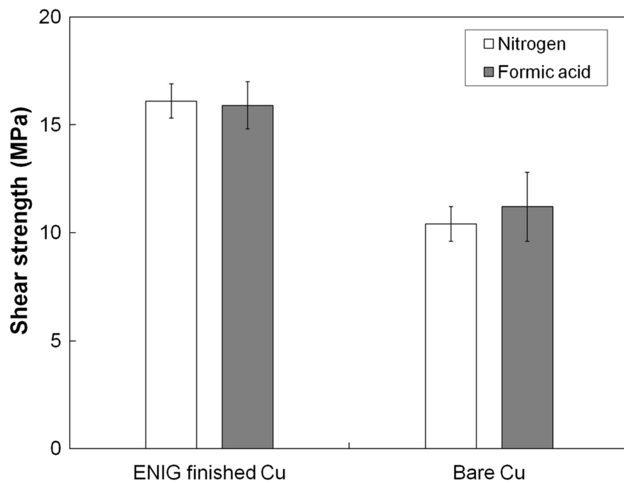

Fig. 8 Shear strength of Ag paste sintered at 300 °C for 60 min in N_2 and formic acid atmosphere without pressure using different substrate

ENIG substrate are shown in Fig. 9a, b. In the fracture surface of the ENIG substrate, Ag was uniformly distributed at both top and bottom. This result could be the evidence indicating that the fracture occurred at the Ag layer. In contrast, the fracture surface of the bare Cu substrate had the Ag and Cu region shown in Fig. 9c, d. The Cu region at the fracture surface means that the fracture position would be different from ENIG substrate. This difference of fracture position would have affected the shear strength. There could be two possibilities for the low shear strength at the bare Cu substrate. One is the presence of oxygen on the Cu surface, and the other is the difference in microstructure at the joint interface caused by surface diffusion between Ag and the substrate. In the case of Cu oxidation, small oxygen regions were observed at the top fracture surface on the Cu substrate (white arrows in Fig. 9c). However, according to Ogura's study, the shear strength of bare Cu to Cu joints sintered at 350 °C without applied pressure had similar values of 11–12 MPa regardless of the atmosphere of N_2 or air [9]. Despite the observed Cu oxide layer, there was no effect on shear strength. In common with this study, the fracture surfaces of Cu joints sintered in N_2 showed both Ag layers and interfacial fractures. Also, Goldmann's research group reported that a Cu oxide layer was not a significant factor in the formation of Cu–Ag inter-diffusion layers for strong bonding [24]. In this study, the shear strength of bare Cu joints in the formic acid atmosphere showed a similar value

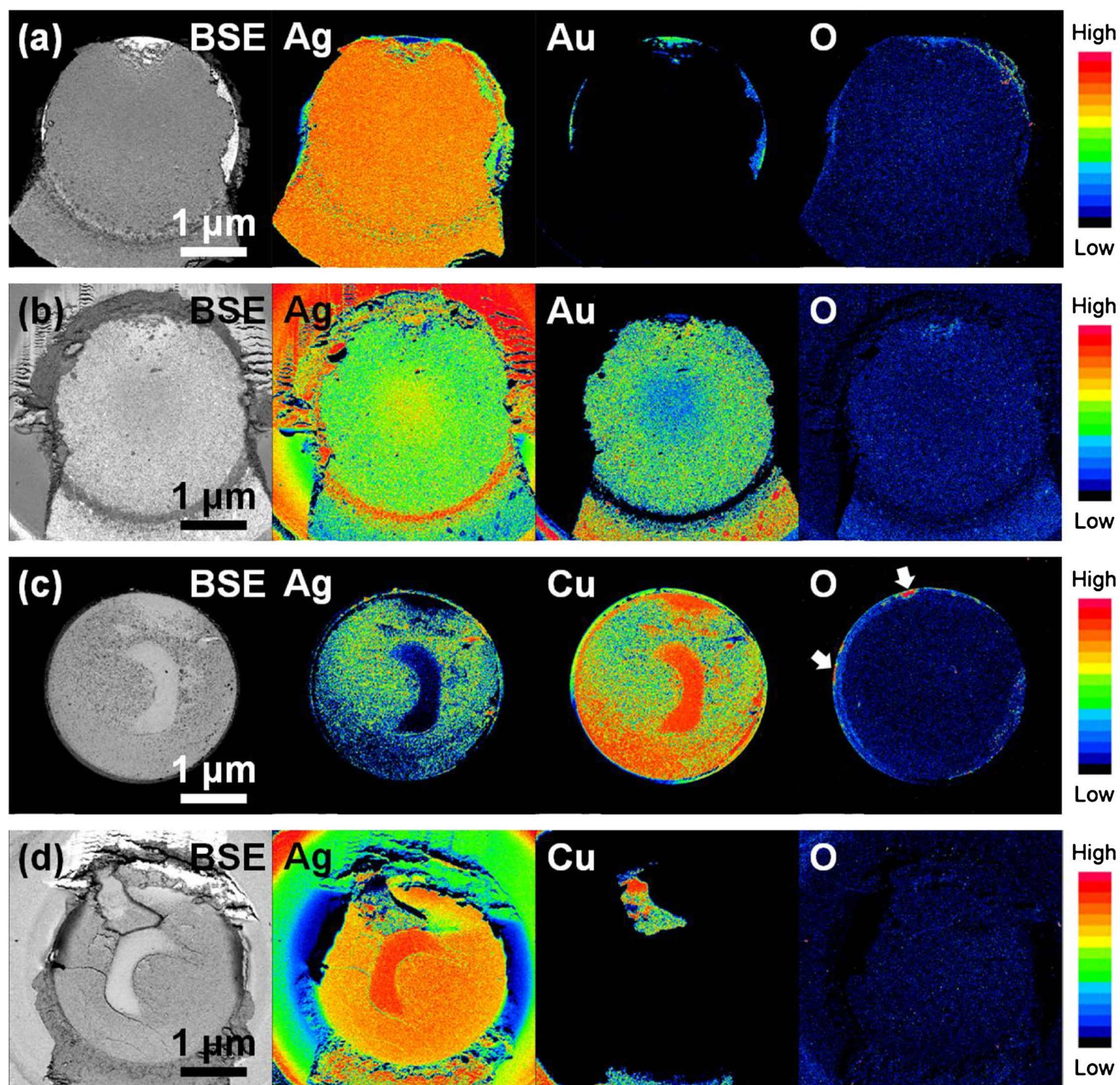

Fig. 9 Typical fracture surfaces of joints bonded at 300 °C for 60 min in N_2 by EPMA mapping: **a** top and **b** bottom of ENIG substrate, **c** top and **d** bottom of bare Cu substrate

to that in N_2 and had still lower value than that of the ENIG finished Cu joint. Formic acid atmosphere is used to reduce surface oxides on Cu and this is effective in removing the natural oxide film that can form during sample preparation before heating. Based on the present observations and other reported results, it seems that the presence of oxide in bare Cu joints was not a major cause of low strength compared to ENIG finished Cu joints.

In order to confirm the other possibility for the strength difference between ENIG finished Cu and bare Cu joint, the microstructure at the joint interface was analyzed. Typical cross-sections of sintered Ag layers on ENIG finished and bare Cu are exhibited in Fig. 10. As shown in Fig. 10a, b, similar sintered Ag morphology was observed regardless of the substrate type. The Ag area ratios of ENIG finished and bare Cu, calculated by cross-section analysis, showed no significant difference (60.1 and 59.4%, respectively). However, the bonding ratio of the ENIG finished Cu substrate had a higher value of 64.1% compared to 40.9% for the bare Cu, in spite of the existence of similar numbers of Ag particles near both surfaces. Also, the contact angle between Ag particles and substrates showed different behavior depending on the substrate type (as shown in Fig. 10c, d). The contact angle of Ag particles to ENIG finished Cu was less than 90°, whereas that on bare Cu was more than 90°. The contact angle could be one of the factors that determines the bonding strength, because a small contact angle generally means a large contact area in the same sized particles. On the other hand, a small contact area with a large contact angle could be a weak spot for fracture.

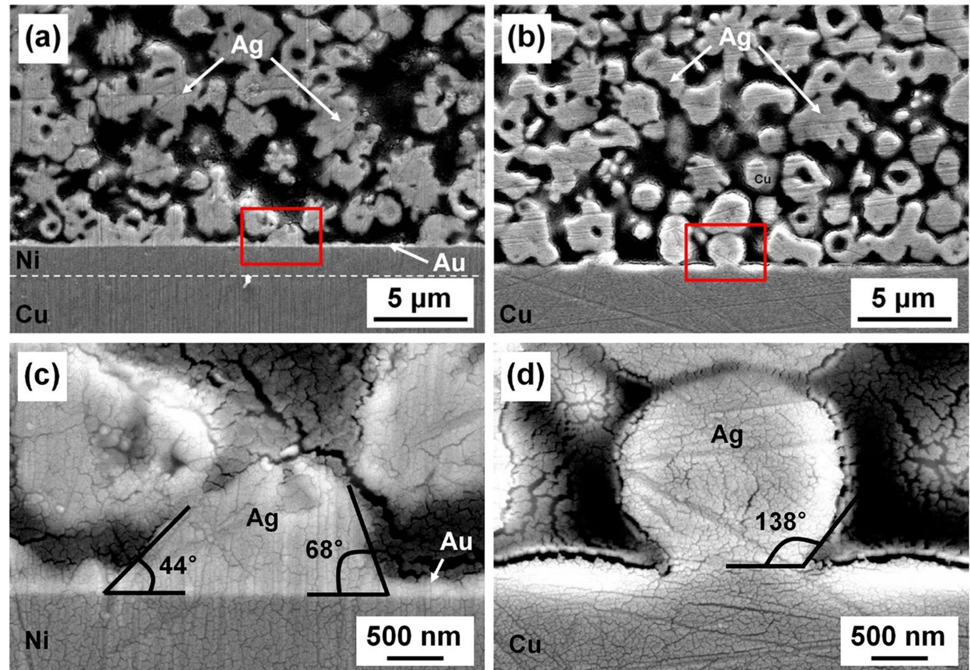

Fig. 10 Cross-section images of sintered Ag layers at 300 °C for 60 min in N_2 on **a** ENIG finished Cu, **b** bare Cu, **c** higher magnification of **a**, and **d** higher magnification of **b**

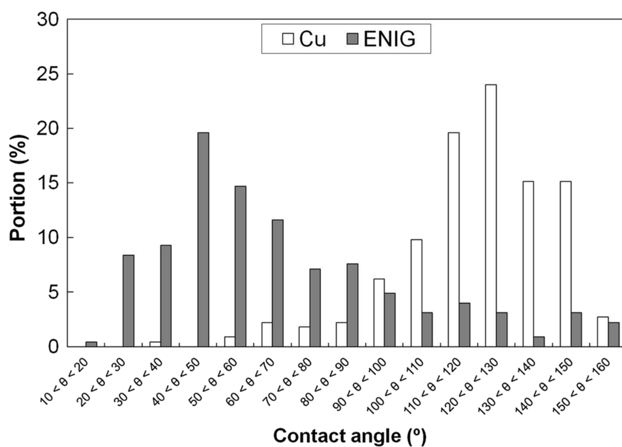

Fig. 11 Contact angle distribution of Ag particles sintered at 300 °C for 60 min in N_2 according to substrate type

Figure 11 shows the contact angle distribution of Ag particles on both ENIG finished and bare Cu substrates. In the case of the ENIG finished Cu substrate, 80% of the contact angles was less than 90°. In contrast, 90% of the contact angles on bare Cu was more than 90°. This difference in contact angle distribution could have affected the bonding ratio, even though the number of Ag particles bonded to substrate was similar. As a result, the fracture surface on ENIG finished Cu showed a uniform Ag region but the Ag joint on bare Cu had an irregular fracture surface with Ag and Cu regions (see Fig. 9).

Figure 12 shows the fracture surface of the top Cu disk in detail. Figure 12a displays the entire fracture surface again. In Fig. 12b, there were some sintered Ag clusters on the fracture surface (Type 2 fracture) and this meant that the fracture mainly occurred at sintered Ag layer. However, lots of Type 1 fracture, which occurred at Ag particles bonded to the Cu substrate, were observed in Fig. 12c, d. Although this area didn't seem to be bonded in Fig. 9c, Ag particles were bonded to the Cu substrate, but the respective contact areas between Ag particles and Cu substrate were small. As mentioned above, we consider that these small contact areas are one reason for low shear strength of joint using Cu substrate.

Although the exact reason why the difference behavior of contact angle occurs is not clear, one possible reason is that the diffusion of Ag on ENIG finished Cu is easier than that on bare Cu. Diffusion is the primary mechanism for sintering and surface chemical reactions. In particular, the diffusion of atoms and molecules on the surface of metal substrates is an important phenomenon for surface-related mass transport. Several studies about the surface diffusion of heterogeneous adatom and surface system, such as Ag/Cu and Cu/Ag, have been undertaken [25–27]. They reported that the adatom is diffused by a jump or an exchange process. Although the dominance of process depended on the system (for example, the simple jump for Ag/Cu and the exchange process for Cu/Ag), it was a common factor that the dominant process had the lowest diffusion barrier. Sanders et al. investigated the diffusion rate on the fcc metal surface for adatom/substrate combinations of Ni, Cu, Rh, Pd, Ag, Pt, and Au [27]. According to their analysis, Ag adatoms were predicted to have smallest diffusion barrier relative to all of the substrates, and they found

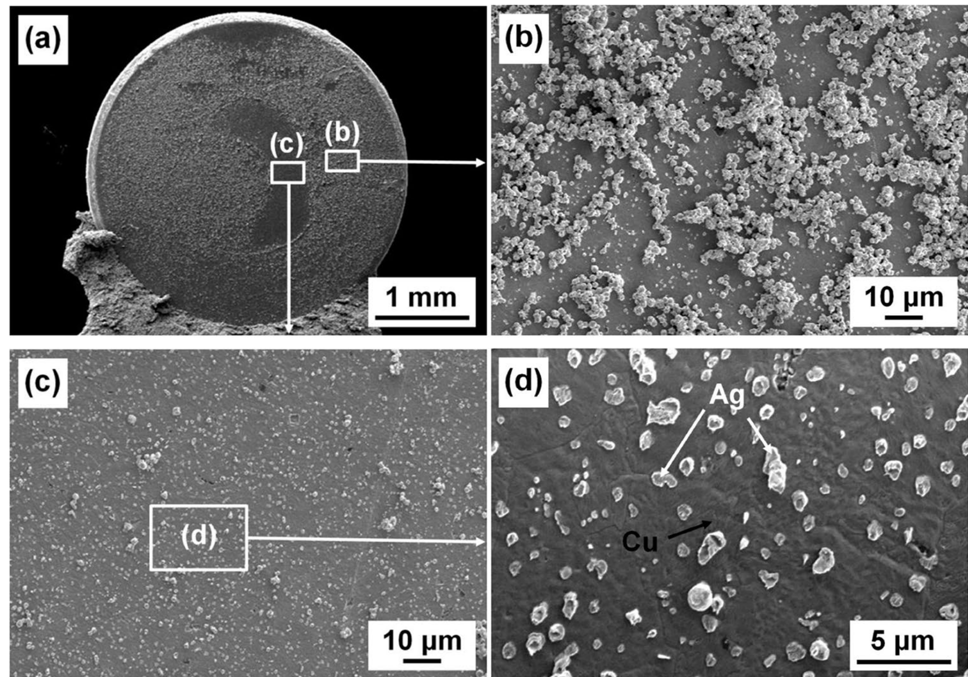

Fig. 12 Fracture surface of the top Cu disk. **a** Entire fracture surface, **b** and **c** high magnification of **a**, and **d** high magnification of **c**

that the diffusion barrier of Ag on Cu substrate showed a higher value than that on Au substrate. This indicated that Ag atoms were easier to diffuse on a Au substrate than Cu substrate. Therefore, it would be possible that the contact angle of Ag on ENIG finished Cu would be smaller than that on bare Cu despite the same bonding process.

4 Conclusions

Ag paste composed of only micro-sized particles was used for high temperature bonding. Even using a pressureless process, bonding by micro-sized Ag particle paste was successfully achieved. The effect of temperature and substrate on shear strength was studied and the main results are summarized as follows:

1. After sintering at temperatures of 250–400 °C for 60 min, CBL Ag particles have almost become spherical in shape and interconnections between Ag particles were observed.
2. The average shear strength of ENIG finished Cu joints increased to 16.1 MPa up to a sintering temperature of 300 °C, and showed similar value above 300 °C.
3. The shear strength of ENIG finished Cu joints was better than that of bare Cu. Although the Ag area ratio of joint layer on both substrates was similar, the bonding ratio on ENIG finished Cu was approximately 25% higher than that on bare Cu.
4. A smaller contact angle of Ag particles on ENIG finished Cu resulted in a larger bonding area, which led to improvement in the bonding strength at the interface compared to the bare Cu substrate.

Acknowledgements This work is supported by Adaptable and Seamless Technology Transfer Program through target-driven R&D, JST.

References

1. K.S. Moon, H. Dong, R. Maric, S. Pothukuchi, A. Hunt, Y. Li, C.P. Wong, J. Electron. Mater. **34**(2), 168–175 (2005)
2. E. Ide, A. Hirose, K.F. Kobayashi, Mater. Trans. **47**, 211–217 (2006)
3. C.A. Lu, P. Lin, H.C. Nin, S.F. Wang, Jap. J. Appl. Phys. **45**(9A), 6987–6992 (2006)
4. J.G. Bai, Z.Z. Zhang, J.N. Calata, G.Q. Lu, IEEE Trans. Compon. Packag. Technol. **29**(3), 589–593 (2006)
5. H. Schwarzbauer, R. Kuhnert, IEEE Trans. Ind. Appl. **27**(3), 93–95 (1991)
6. J. Yan, G. Zou, A. Wu, J. Ren, J. Yan, A. Hu, Y. Zhou, Scr. Mater. **66**, 582–585 (2012)
7. S. Wang, M. Li, H. Ji, C. Wang, Scr. Mater. **69**, 789–792 (2013)
8. T. Wang, X. Chen, G.Q. Lu, G.Y. Lei, J. Electron. Mater. **36**(10), 1333–1340 (2007)
9. H. Ogura, M. Maruyama, R. Matsubayashi, T. Ogawa, S. Nakamura, T. Komatsu, H. Nagasawa, A. Ichimura, S. Isoda, J. Elecron. Mater. **39**(8), 1233–1240 (2010)
10. T.G. Lei, J.N. Calata, G.Q. Lu, IEEE Trans. Compon. Packag. Technol. **33**(1), 98–104 (2010)
11. K.S. Siow, J. Alloy. Compd. **514**, 6–19 (2012)
12. Y. Akada, H. Tatmumi, T. Yamaguchi, A. Hirose, T. Morita, E. Ide, Mater. Trans. **49**(7),1537–1545 (2008)
13. W.H. Li, P.S. Lin, C.N. Chen, T.Y. Dong, C.H. Tsai, W.T. Kung, J.M. Song, Y.T. Chiu, P.F. Yang, Mater. Sci. Eng. A **613**, 372–378 (2014)

14. Z. Zhang, G.Q. Lu, IEEE Trans. Electron. Packag. Manuf. **25**(4), 279–283 (2002)
15. H. Nishikawa, X. Liu, X. Wang, A. Fujita, N. Kamada, M. Saito, Mater. Lett. **161**, 231–233 (2015)
16. S. Sakamoto, S. Nagao, K. Suganuma, J. Mater. Sci. **24**, 2593–2601 (2013)
17. K. Suganuma, S. Sakamoto, N. Kagami, D. Wakuda, K.S. Kim, M. Nogi, Microelectron. Reliab. **52**(2), 375–380 (2012)
18. M. Kuramoto, S. Ogawa, M. Niwa, K.S. Kim, K. Suganuma, Die bonding for a nitride light-emitting diode by low-temperature sintering of micrometer size silver particles. IEEE Trans. Compon. Packag. Technol. **33**(4), 801–808 (2010)
19. M. H. Roh, H. Nishikawa, S. Tsutsumi, N. Nishiwaki, K. Ito, K. Ishikawa, A. Katsuya, N. Kamaka, M. Saito, Pressureless bonding by micro-sized silver particle paste for high-temperature electronic packaging, Mater. Trans. **57**(7), 1209–1214 (2016)
20. J.S. Reed, *Principles of Ceramics Processing*, 2nd edn. (Wiley, New York, 1995)
21. Y.C. Lin, J.H. Jean, J. Am. Ceram. Soc. **87**(2), 187–191 (2004)
22. H. Suzuki, Solution hardening in Au-Ag and Cu-Ni alloy crystals, in *Strength of Metals and Alloys (ICSMA 8)*, ed. by P.O. Kettunen, T.K. Lepisto, M.E. Lehtonen (Pergamon Press, Oxford, 1988), pp. 573–578
23. M.S. Kim, H. Nishikawa, Silver nanoporous sheet for solid-state die attach in power device packaging. Scr. Mater. **92**, 43–46 (2014)
24. U. Kürpick, G. Meister, A. Goldmann, Appl. Surf. Sci. **99**(3), 221–227 (1996)
25. K. Sbiaai, Y. Boughaleb, M. Mazroui, A. Hajjaji, A. Kara, Thin Solid Films **548**, 331–335 (2013)
26. E. Elkoraychy, K. Sbiaai, M. Mazroui, Y. Boughaleb, R. Ferrando, Surf. Sci. **635**, 64–69 (2015)
27. D.E. Sanders, A.E. DePristo, Surf. Sci. **260**, 116–128 (1992)